

Contents lists available at ScienceDirect

Journal of Science: Advanced Materials and Devices

journal homepage: www.elsevier.com/locate/jsamd



Research Article

Magnetic and pH-Sensitive dual actuation of biohybrid microswimmer of targeted drug release suitable for cancer cell microenvironment

Richa Chaturvedi ⁺, Yumin Kang ⁺, Yunji Eom, Sri Ramulu Torati ¹, CheolGi Kim ^{*}

Department of Physics and Chemistry, DGIST, Daegu, 42988, Republic of Korea

ARTICLE INFO

Keywords: Magnetotactic bacteria Magnetic microswimmer Lenalidomide Drug delivery

ABSTRACT

The chemotherapeutic agents most frequently used in cancer treatment often have limited effectiveness because of their low specificity for tumors and poor therapeutic performance. In addition to the aforementioned therapeutic challenges the drug delivery carriers conjugated with the drug encounter early detection and elimination from the immune system before arriving at the affected area continues to be a significant research focus among researchers. To address this prevalent issue, an effective approach has been developed that leverages the physiological differences between normal and tumor tissue to enhance the efficacy of anticancer drugs. This drug delivery system is designed based on pH-sensitive drug release, ensuring targeted release within cancer cells. In the present study, we have developed a drug carrier called as biohybrid magnetic microswimmer (BMM). The BMM was formed through a three-step process: firstly, bacterial surfaces were functionalized with biotinylated PEG which enables the bacteria to escape the phagocytosis process; secondly, the anticancer drug lenalidomide was PEGylated to enhance solubility; and finally, both complexes were conjugated via streptavidin-biotin interaction. The study investigated bond formation, bacterial viability after drug treatment, pH-dependent release, and cytotoxicity in various cell lines (MCF-7 and THP-1 cells), and the results revealed that the concentration of the drug, released from BMM gradually increased as the pH of the solvent decreased from neutral to acidic, mimicking the surrounding environment of normal cells and cancer cells, respectively, which in turn affects the cancer cell viability negatively. Therefore, BMM shows promise in targeted drug delivery, utilizing magnetic manipulation and pH-triggered release, providing advantages that include bacteria's maneuverability and PEG's stealth properties, enhancing drug efficacy.

1. Introduction

Currently, cancer stands as the predominant and widespread cause of mortality globally. There are various types of cancer treatments available, including chemotherapy, radiation, immunotherapy, and surgery. Among all these therapies, chemotherapy is the most widely used [1–3]. Although chemotherapy is the most used treatment modality, chemotherapeutic agents and drugs often fall short in the process due to their properties, such as low tumor targeting, low therapeutic efficacy, poor biodistribution, limited solubility, and cytotoxicity to normal cells and tissues. These shortcomings can lead to treatment delays or, sometimes, failure in cancer treatment. Currently, many nanotechnologies-based drug delivery systems are being trialed and studied for specific targeted delivery of drugs to the cancer site in order to improve the

treatment process by enhancing the biodistribution, increasing solubility, and internalization while minimizing the side effects of the drugs [4-8].

Despite advancements in bioengineered drug delivery systems, inefficient drug release within tumor cells remains a major challenge, significantly reducing therapeutic efficacy [9]. To overcome this, a triggered drug release system has been developed, enabling controlled drug release in response to external and internal stimuli such as temperature, pH, and enzymatic activity [10]. Unlike other conventional methods of drug delivery and release. Stimuli-responsive drug delivery systems release their payload upon detecting specific triggers, ideally at the diseased site, to enhance therapeutic efficacy while reducing the adverse effects of the active pharmaceutical ingredient, thereby minimizing side effects for patients [11,12]. The distinct extracellular acidic

E-mail address: cgkim@dgist.ac.kr (C. Kim).

https://doi.org/10.1016/j.jsamd.2025.100873

^{*} Corresponding author.

⁺ Equally contribute to the paper.

¹ Present address: Center for Bioelectronics, Old Dominion University, Norfolk, VA- 23508, USA.

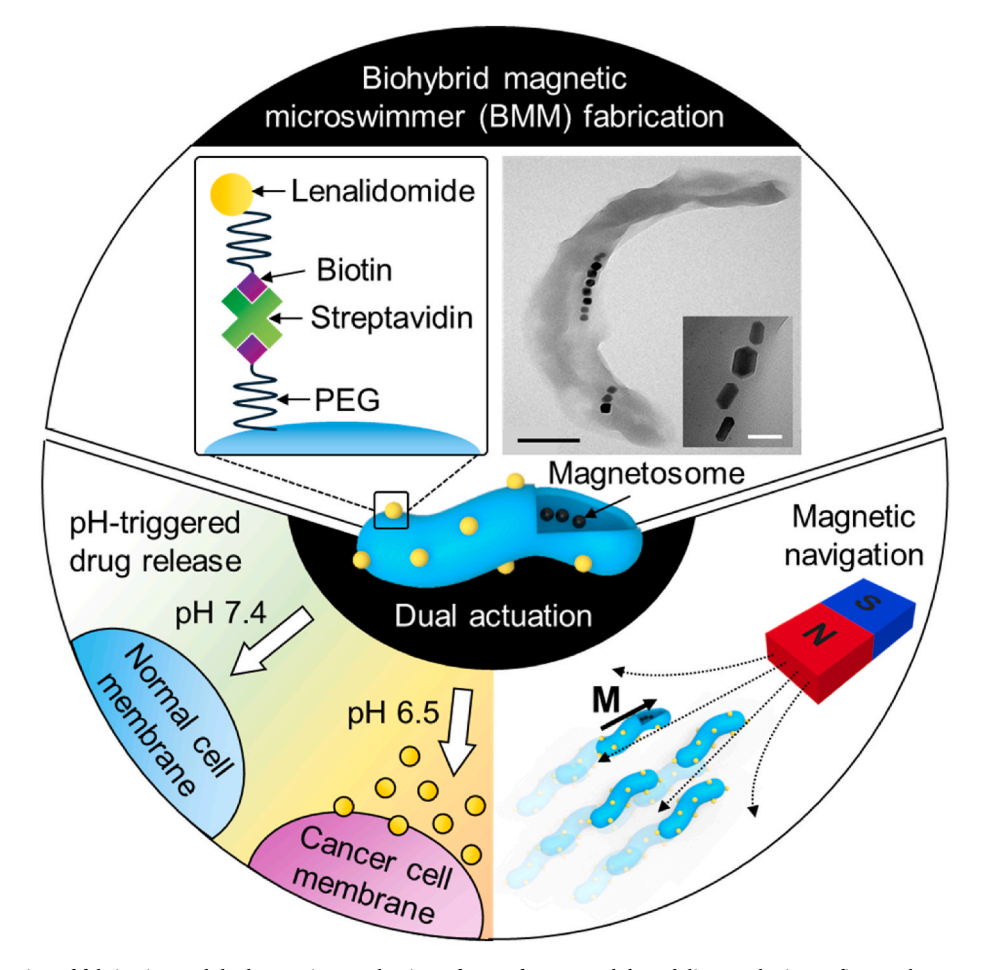


Fig. 1. Schematic illustration of fabrication and dual actuation mechanism of BMM for targeted drug delivery. The insert figures show TEM image of the structural morphology of MTB and the magnetosomes that developed within the bacterial cell (Scale bar: 200 nm (black), and 50 nm (white)).

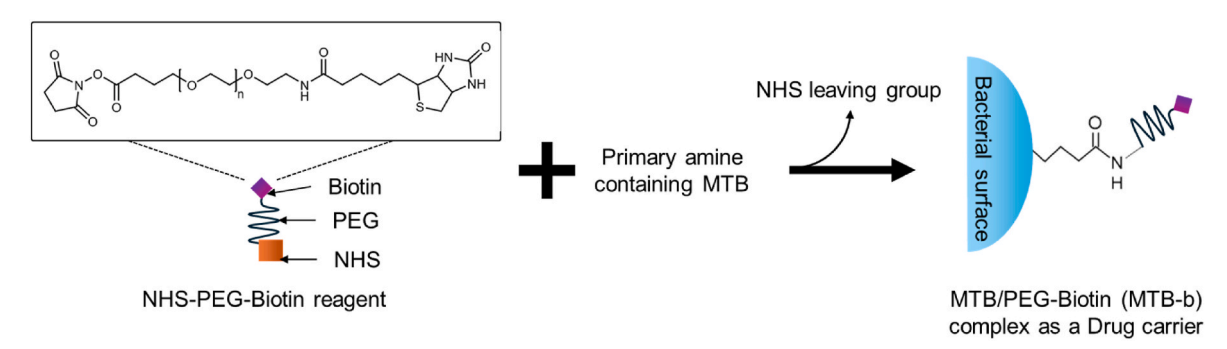


Fig. 2. Schematic illustration for loading of PEG-biotin on the bacterial surface. The MTB/PEG-biotin (MTB-b) was a result of an amide bond formation between the primary amines present on the surface of the bacteria and the NHS group present in the PEG-NHS-biotin reagent via a nucleophilic attack and by releasing a NHS group.

and intracellular alkaline environments of cancer cells facilitate precise drug release within the tumor microenvironment.

Among various nanotechnology-based approaches, bio-conjugated and bioengineered bacteria have garnered significant interest as versatile drug delivery systems, offering enhanced pharmaceutical efficacy in targeted drug delivery [13,14]. Many micro- and nano-swimmers have been explored as promising carriers for cancer therapy [15,16]. Bio-functionalized and bioengineered bacteria, loaded with artificial cargo, serve as effective drug delivery devices due to their unique properties, including self-propulsion, triggered drug release, small size, ease of bioconjugation, and passive tumor localization [17–21]. Additionally, bacterial drug delivery systems can undergo surface

modifications through ligand or antibody attachment for enhanced targeting [22–24].

Amid the various bacteria employed in drug delivery, magnetotactic bacteria (MTB) offer a compelling alternative owing to their capacity to detect and navigate toward hypoxic regions, a defining feature of cancerous tumors, facilitating targeted drug delivery while enabling stimuli-responsive drug release [25,26–29]. Also, MTB exhibit self-propulsion, facilitated by the presence of magneto-somes—intracellular magnetic nanoparticles [30]. Additionally, various nanoparticles, including polymeric, inorganic, and lipid-based types, are employed in drug delivery systems due to their unique characteristics, such as stability, biodistribution, and ease of modification [31].

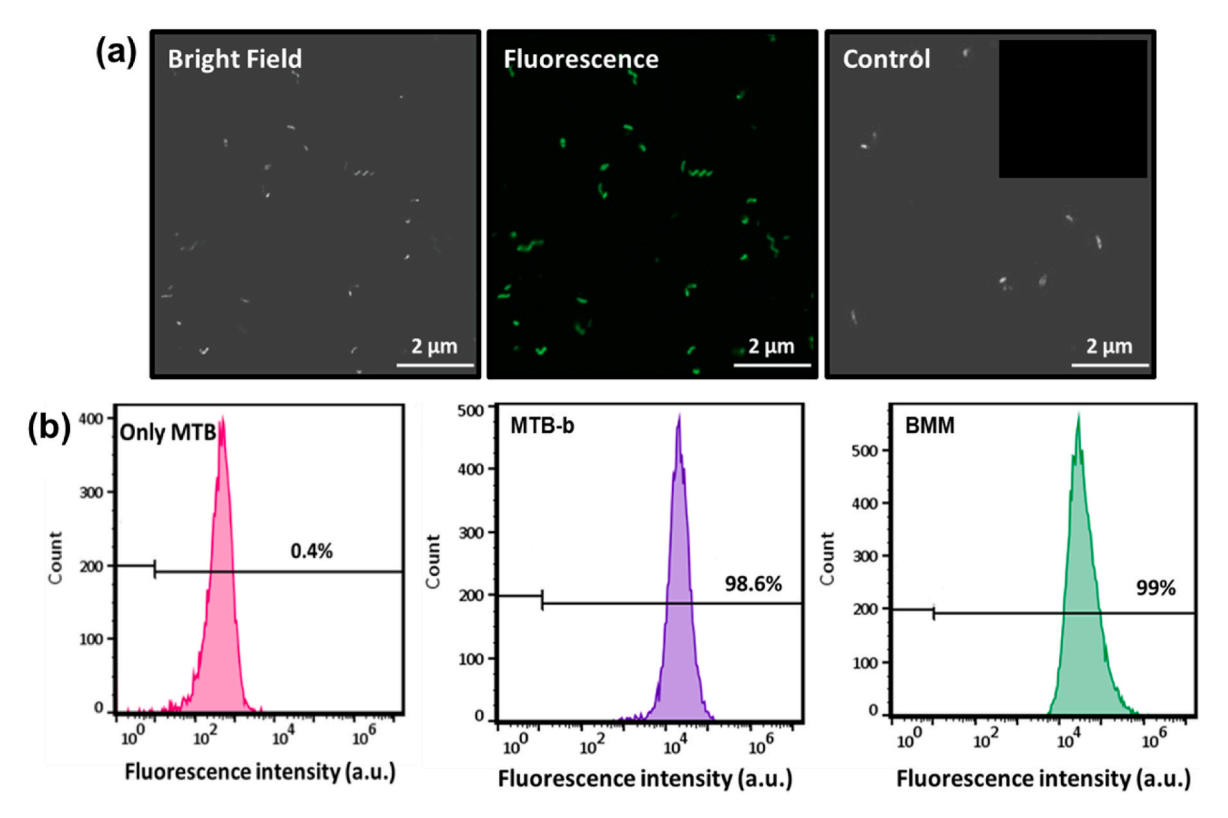


Fig. 3. Verification of the drug attachment with BMM. (a) Confocal microscopy images present the bright field and fluorescence views of the FITC-labeled BMM with unlabeled MTB serving as the control (insert: fluorescence view of control group). (b) FACS histogram obtained from only MTB, MTB-b and BMM demonstrate that the drug lenalidomide (LENA) is uniformly attached to the MTB-b in a sandwich-like arrangement.

However, drug delivery systems often face phagocytic attack, which can limit their effectiveness. In addition to challenges posed by phagocytosis, drug delivery systems also struggle with low solubility. To address this, various materials such as chitosan, cyclodextrins, and PEG are incorporated to enhance the solubility of hydrophobic drugs [32]. Among the previously mentioned materials, PEG holds an advantage over chitosan, as it not only enhances drug solubility and helps evade phagocytosis but is also recognized for its water-resistant properties, whereas chitosan lacks strong water resistance [33].

Additionally, biotin and NHS play a crucial role in bioconjugation and maintaining drug stability. Biotin, an essential vitamin for bacterial survival, has been demonstrated to efficiently load and bind various anticancer drugs through bioconjugation techniques [34]. In the recent times, Biohybrid Magnetic Microswimmers (BMMs) have emerged as a promising platform for biomedical applications [35,36]. These microscopic robots are engineered by integrating biocompatible materials such as microorganisms or cells, with magnetic actuation mechanisms and therapeutic agents.

In this article, we present a dual actuation system for targeted drug delivery, employing BMMs fabricated with therapeutic agents and functionalized MTBs. The position manipulation and selective drug release were demonstrated to enhance the efficiency of targeted drug delivery using magnetic and pH-sensitive dual actuation. Firstly, the locomotion of MTBs was investigated under a streamlined magnetic field generator based on their intrinsic magnetic property. Moreover, the MTB bacteria were functionalized by attaching to the biotinylated PEG. This attachment not only aids in shielding the drug delivery system from phagocytosis for better biodistribution of drug but also provides a robust platform for the conjugation of lenalidomide (LENA) drug. The cancer drug lenalidomide was chosen to be coupled with the drug carrier MTB-b for the following reasons: (1) Lenalidomide is clinically relevant and widely prescribed for the treatment of cancer due to its classification as a potent immunomodulatory drug [37], (2) the solubility of lenalidomide

is pH-dependent, (3) the drug's structure features a primary amine functional group, which facilitates the attachment to the drug delivery carrier through a covalent bonding [38], and (4) this drug can be administered over an extended duration as it reduces the risk of new cancer by attacking the abnormal cancer cells [39]. Moreover, lenalidomide is a drug that shows potential in treating triple-negative breast cancer (TNBC) when used in combination with other drugs such as cetuximab or trastuzumab. It enhances the activity of natural killer (NK) cells and stimulates them to produce chemokines that attract additional immune cells. Additionally, it can inhibit the NF-κB pathway and reverse tolerance to tumor antigens [40,41]. The drug loading into the drug delivery complex is achieved through a sandwiched reaction method between biotin and streptavidin. The developed drug delivery system is thoroughly assessed for the establishment of a robust conjugation, magnetic manipulation, the viability of bacteria after treatment, pH-dependent drug release in diverse pH environments, as well as the cellular viability of various cell lines.

2. Material and method

2.1. Reagents and chemicals

Magnetospirillm magneticum (ATCC 700264), THP-1 cells (ATCC TIB-202), MCF-7 cells (ATCC HTB-22) bacteria was procured from the American Type Culture Collection (Manassas, VA, USA), Eagle's Minimum Essential Medium (ATCC), Rosewell Park Memorial Institute (RPMI-1640) medium, phosphate-buffered saline (PBS), fetal bovine serum (FBS), Slide-A-Lyzer MINI Dialysis Devices, 10K MWCO, and penicillin and streptomycin were acquired from Thermo Fisher Scientific (Waltham, MA, USA). Live/dead Baclight bacterial viability kits and live/dead viability/cytotoxicity were obtained from Invitrogen (Waltham, MA, USA). (2-(2-methoxy-4-nitrophenyl)-3-(4-nitrophenyl)-5-(2,4-disulfophrnyl)-2H-tetrazolium, Monosodium salt (WST-8) (Cell

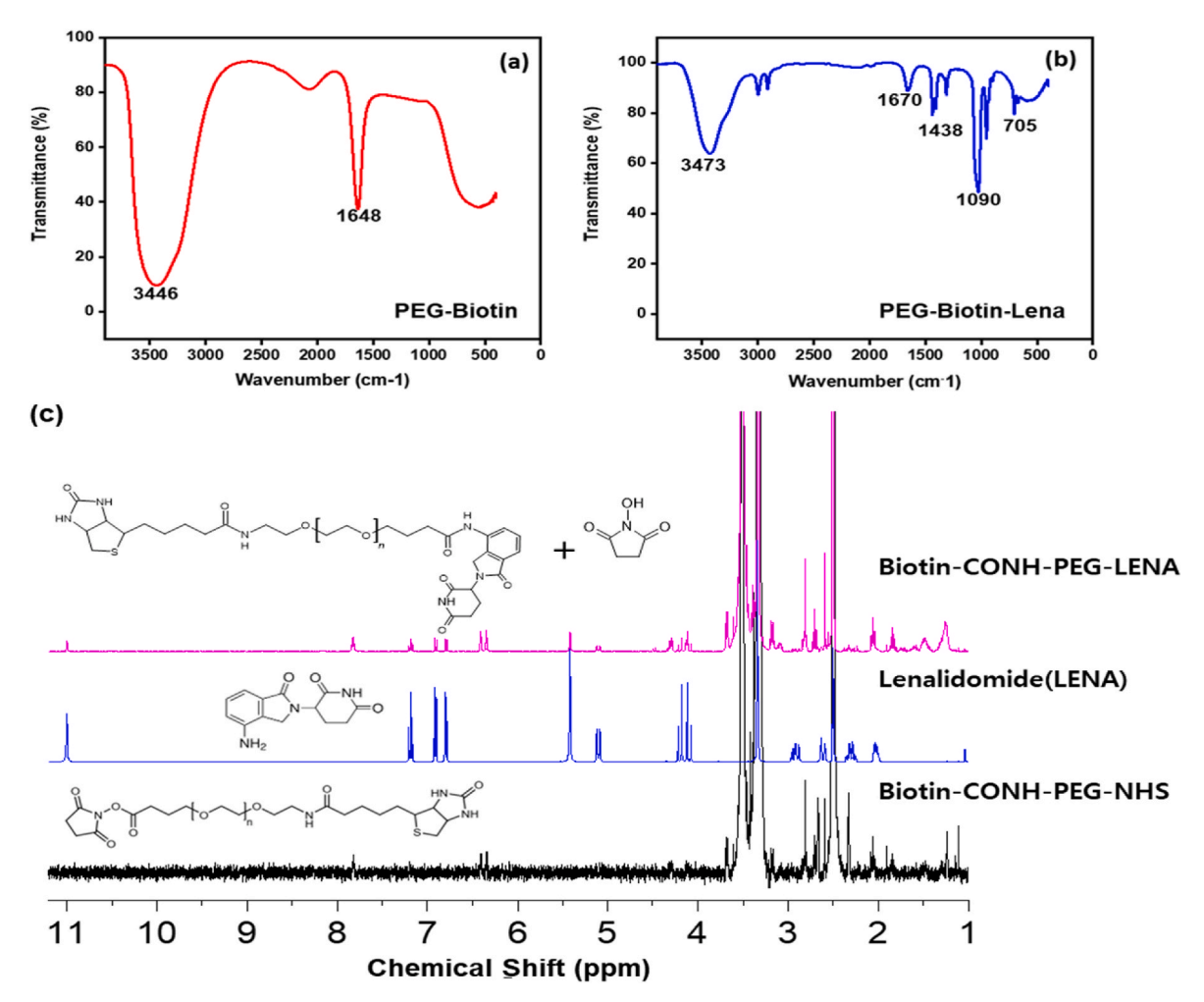


Fig. 4. FT-IR spectrum of (a) PEG-Biotin, (b) PEG-Biotin-LENA drug, and (c) 1H NMR measurement of PEG-Biotin-LENA, Lenalidomide(LENA) and PEG-Biotin.

counting kit-8, CCK-8) was purchased from ENzoLife Sciences, Inc. (Rep. of. Korea). Streptavidin and lenalidomide were acquired from Sigma Aldrich (MS, USA). Biotinylated PEG derivative with a terminal biotin group (Biotin–CONH–PEG-O-C3H6–CONHS) [MW-5000 Da] was purchased from Rapp Polymere GmbH (Tubingen, Germany). Ethanol and methanol were purchased from Daejung Chemicals (Rep. of. Korea). Mili-Q water was obtained from Mili-Q water system (Milipore, Bedford, MA).

2.2. Formation of drug loaded BMM

The development of a drug delivery agent was successfully achieved by implementing a sandwiched reaction involving the drug, the biotin-PEG-NHS reagent, and the bacteria. The bacteria that were utilized to make the drug carrier is a magnetotactic bacteria named Magnetospirillum magneticum AMB-1. Magnetospirillum magneticum AMB-1 from ATCC (ATCC 700264) was cultured microaerobilcally in ATCC (1653) MSGM medium as prescribed previously in our paper [42]. The attachment of the drug to the complex was accomplished through a three-step process. Briefly, the bacteria were bound to the PEG-biotin for the first step. A solution of biotin-PEG-NHS (Rapp Polymere GmbH) at a concentration of 10 mg/mL was prepared in distilled water to create a stock solution of 20 mM. Subsequently, 100 μL of this solution was subjected to incubation with magnetotactic bacteria (MTB) on a rotator for 2 h at room temperature. Finally, the MTB/PEG-biotin complex (MTB-b) was rinsed and dispersed in a PBS solution for further use. In the next step, the lenalidomide drug was attached to the PEG-biotin reagent. To ensure efficient attachment of the drug to the MTB-b, it is

important to note that the lenalidomide drug contains a primary amine in its structure which can be effectively coupled with the biotin-PEG-NHS component found in the tin-CONH-PEG-O-C₃H₆-CONHS reagent in a similar to the attachment of bacteria. In the next step, the lenalidomide drug was coupled with the PEG-biotin reagent as follows: Firstly, an 8 mg/mL concentration of lenalidomide drug was dissolved in DMSO (Daejung Chemicals) to make a stock solution. Then, 500 μL of PEG-biotin was mixed with 100 μL of lenalidomide drug, and the mixture was left on a rotator at room temperature for overnight incubation. The following day, 500 μL of the freshly prepared MTB-b was mixed with 200 μL mixture of Lena/PEG-biotin was mixture and placed on a rotator for 4 h at room temperature. Also, 100 µL of streptavidin (Sigma Aldrich) was added to the mixture to facilitate a biotin-streptavidin bond between the two different mixtures.

2.3. Assessment of BMM

The examination of the prepared drug delivery microrobot was performed via two methods namely, fluorescence microscopy and fluorescence-activated cell sorting (FACS). The fluorescent images of the drug delivery carrier were captured using a confocal laser scanning microscope (Carl Zeiss LSM 800) equipped with a high numerical aperture (NA) 63x1.4 oil immersion objective along with an imaging software (Zeiss ZEN LSM). The FITC-labeled lenalidomide drug conjugated with the MTB-b was analyzed for the formation and characterization of the drug delivery carrier. The labeled BMM was analyzed using fluorescence-activated cell sorting (FACS: BD Accuri C6,

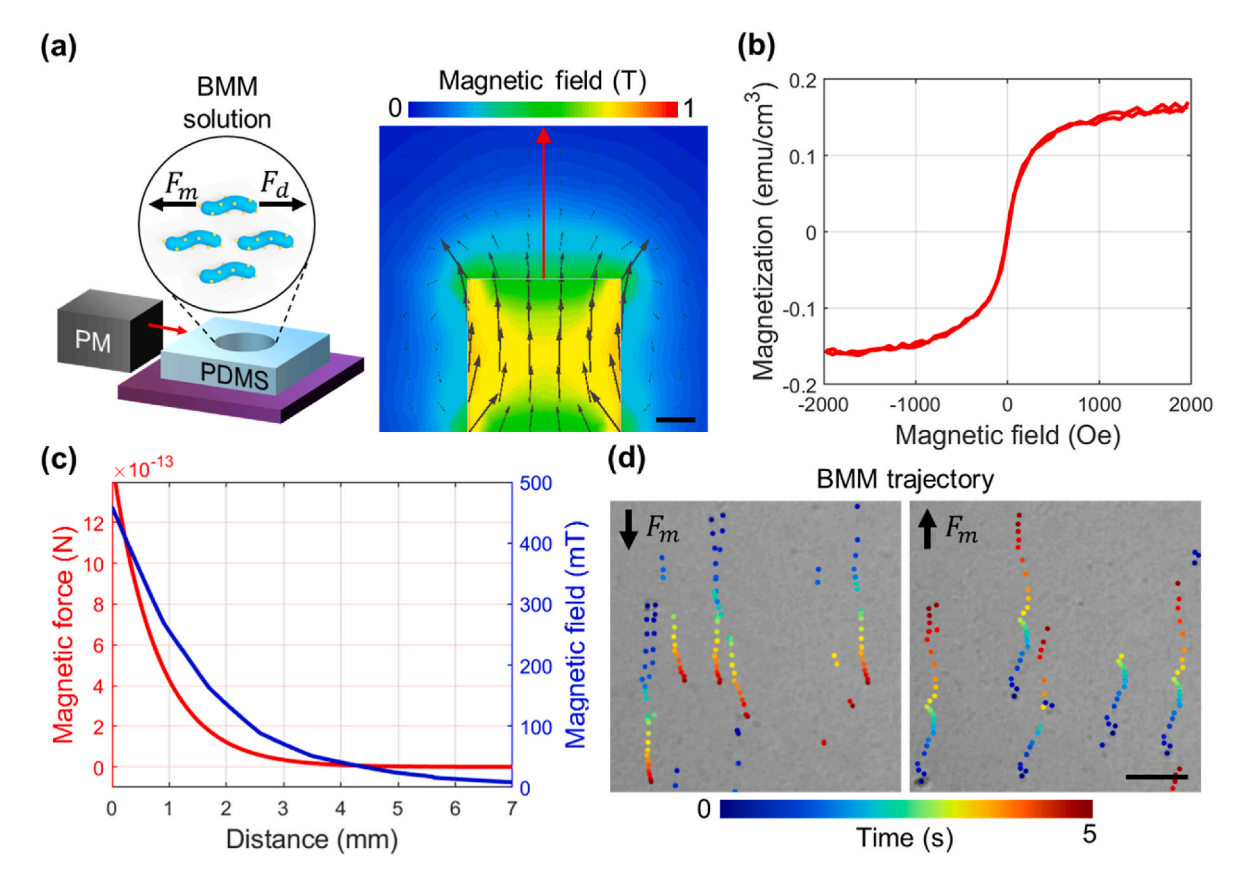


Fig. 5. Magnetic navigation of BMM. (a) BMM manipulation using a simplified magnetic field generator. The magnetic field from the PM was simulated by Ansys Maxwell software (scale bar = 2 mm). The red arrow indicates the direction of the BMM sample. (b) The magnetization measurement of 1 ml of 1% BMM solution was done using a vibrating-sample magnetometer (VSM). (c) Y axial magnetic field and magnetic force were calculated according to the distance from the PM surface, based on the BMM magnetization and magnetic field. (d) Magnetic navigation trace of BMM. Variable colored dots indicate the trajectory according to time (scale bar $= 20 \mu m$).

Biosciences, wavelength of 488 nm). All the samples were formulated in PBS, and the measurements were acquired through forward scatter with 10,000 events for the intensity plots. The outcomes were then analyzed using FlowJo software. The untreated MTB served as the control.

The magnetic properties of BMM were measured using a vibrating sample magnetometer (VSM, FEI Tecnai G2 F20 TWIN TMP) at room temperature. The magnetic field generated from the neodymium magnet was calculated using Ansys Maxwell simulation. The magnetic force (F_m) on the BMM was calculated by following Eq. (1), where the magnetic moment of the magnetic particle is an inhomogeneous magnetic field [43]. Also, the drag force (F_d) of a spherical particle can be calculated based on Stoke's law by following Eq. (2), where is the radius of the particle, is the viscosity of the fluid, and is the velocity of the particle. The drag force exerted on BMMs was estimated by assuming the BMM as a spherical particle with a diameter of 1 μ m and velocity in order of 1 μ m/s, considering the viscosity of water.

$$F_m = (m \bullet \nabla) \mathbf{B}$$
 Eq. (1)

$$F_d = 6\pi\eta r v$$
 Eq. (2)

2.4. Evaluation of MTB viability with Lena drug coupling

To evaluate the viability of MTB after incubation with the lenalidomide drug, a live/dead BacLight bacterial viability kit was used. The kit consists of two different dyes: an SYTO and propidium iodide dye that transmits green-colored fluorescence to the live bacteria and a red-colored fluorescence to the dead bacterial cells respectively. In the given experiment, two types of bare MTB bacteria (live and dead) were used as a control, in addition to a blank containing only lenalidomide. A

concentration of 1×10^5 MTB cells was seeded in a 96-well plate along with various concentrations (10, 20, 30, 40, and 50 µg/mL) of lenalidomide drug and the BMM mixture was then incubated for different time intervals (6, 12, and 24 h). The experiment was performed in triplicates. After the incubation, a solution of live/dead dye was added to the BMM and incubated for 15 min in a dark environment. The live/dead dye mixture was prepared according to the manufacturer's protocol. To measure the fluorescence intensity of the sample a microplate reader (BioTek Synergy H1) was used, and to capture the fluorescence images of the live and dead bacterial cells after an incubation of 6 h, an inverted fluorescence microscope (OLYMPUS IX83) was used.

2.5. THP-1 and MCF-7 cell culture

For the present study, two types of cell lines were used to check the effectiveness of drug and drug delivery agents. THP-1 (ATCC TIB-202) cells were propagated in RPMI 1640 medium (Thermo Fisher Scientific) as specified by the manufacturer. MCF-7 (ATCC HTB-22) cells were cultivated in DMEM medium following the manufacturer's recommended conditions. In both the cell culture media, 1% penicillin/streptomycin and 10% FBS solution was added to prevent any kind of contamination. The cells were incubated in a humidified incubator at 37 $^{\circ}\text{C}$ temperature with 5% CO $_2$ for a duration of 2–3 days. Since MCF-7 cells adhere to the culture flasks, they were detached using a Trypsin-EDTA solution before proceeding with the experiments.

2.6. pH-dependent lenalidomide drug release

The analysis of pH-activated drug release of the drug lenalidomide

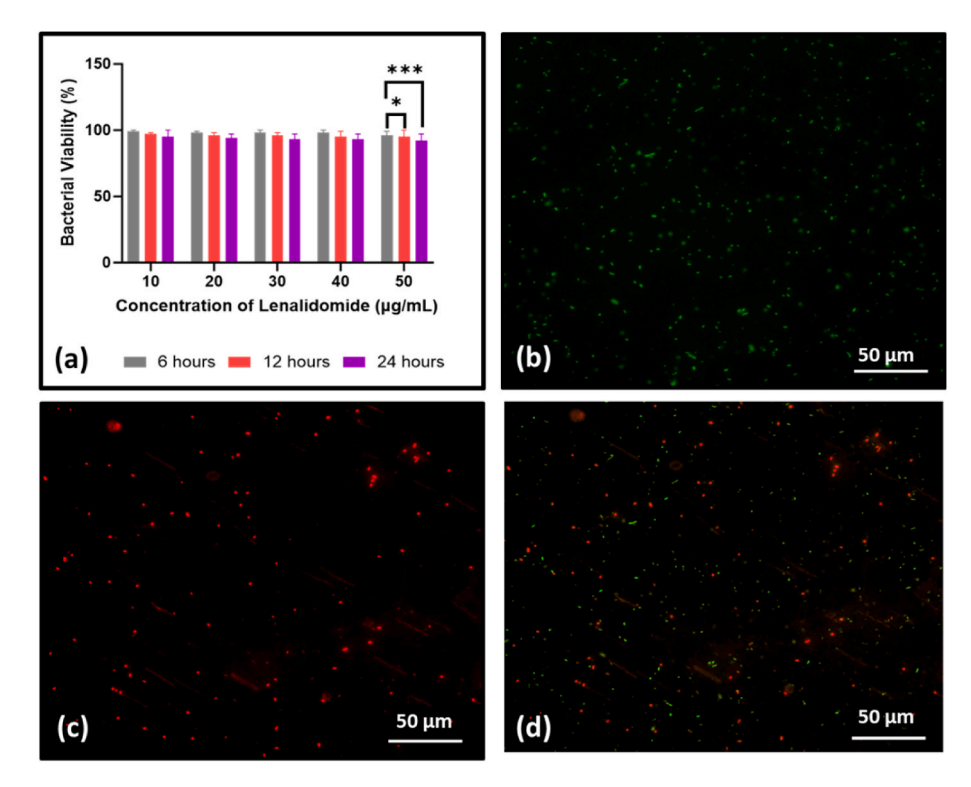


Fig. 6. BMM bacterial viability. (a) Evaluation of MTB bacterial viability was conducted by exposing the bacteria to various concentrations of the drug Lenalidomide (Lena) (10, 20, 30, 40, and 50 μ g/mL) for different durations (6, 12, and 24 h). The results demonstrate minimal bacterial cell damage even after a 24-h incubation with most bacteria alive, even at higher drug concentrations. Data is represented as mean \pm SD, n=3. Statistical significance is denoted with * for P < 0.01 and *** for P < 0.001, indicating significant differences between data sets at 6, 12, and 24 h. (b) Fluorescent microscopy images showing live bacterial cells stained with SYTO stain, (c) Microscopy images depicting dead bacterial cells stained with propidium iodide, and (d) a merged image of live and dead bacterial cells.

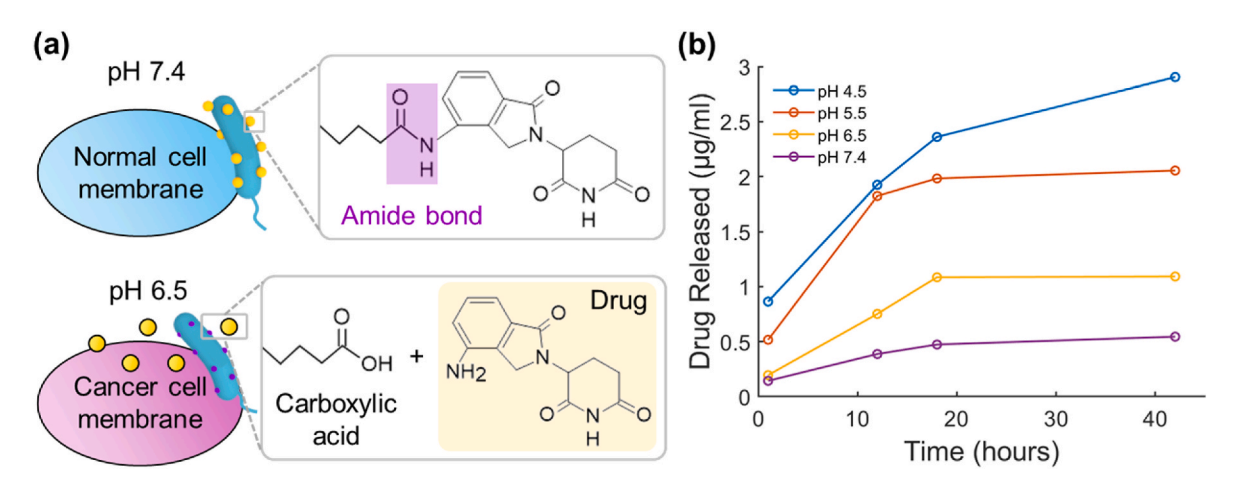


Fig. 7. Investigation of pH-dependent drug release from BMM (a) Mechanism of drug release under the acidic condition. The amide bond in the conjugated Drug-PEG complex is broken into carboxylic acid and amine by hydrolysis process. (b) Lenalidomide release over time from BMM at different pH values (4.5, 5.5, 6.5, and 7.4).

(Sigma Aldrich) from the drug carrier was achieved as follows: BMM (0.5 mL, 3 mg/mL) was loaded into a dialysis device (Slide A Lyzer MINI Dialysis Device, 10KMWCO), and then these devices were placed inside 15 mL conical tubes containing 14 mL of PBS of different pH (4.5, 5.5 6.5 and 7.4). The BMM was incubated for specified time intervals (1h, 12h, 18h and 42 h) and after incubation the samples were collected from the dialysis buffer, and the dialysis buffer was replenished with an equivalent volume of fresh buffer. The quantification of lenalidomide release was carried out on the collected samples by measuring absorbance using a UV–visible spectrophotometer at 310 nm wavelength [44].

2.7. CCK-8-based cytotoxicity assay

We assessed the cytotoxic effects of MTB-b and the unmodified BMM on various cell lines using CCK-8 assay. In the present study, THP-1 and MCF-7 cells were initially pipetted out in a 96-well plate at a concentration of $2x10^5$ and incubated under optimized conditions. Both cell lines were treated with MTB-b and BMM at concentrations of 20 mM and 50 μ g/mL, respectively and the untreated cells were kept as a control. Following an incubation of 24 h, 10 μ L of CCK-8 solution was introduced to the cell, and MTB-b and BMM mixture. The plates were then incubated in a humidified incubator at 37 °C for an additional time of 2 h. As per the principle of CCK-8 assay, the exposed cells produce a formazan

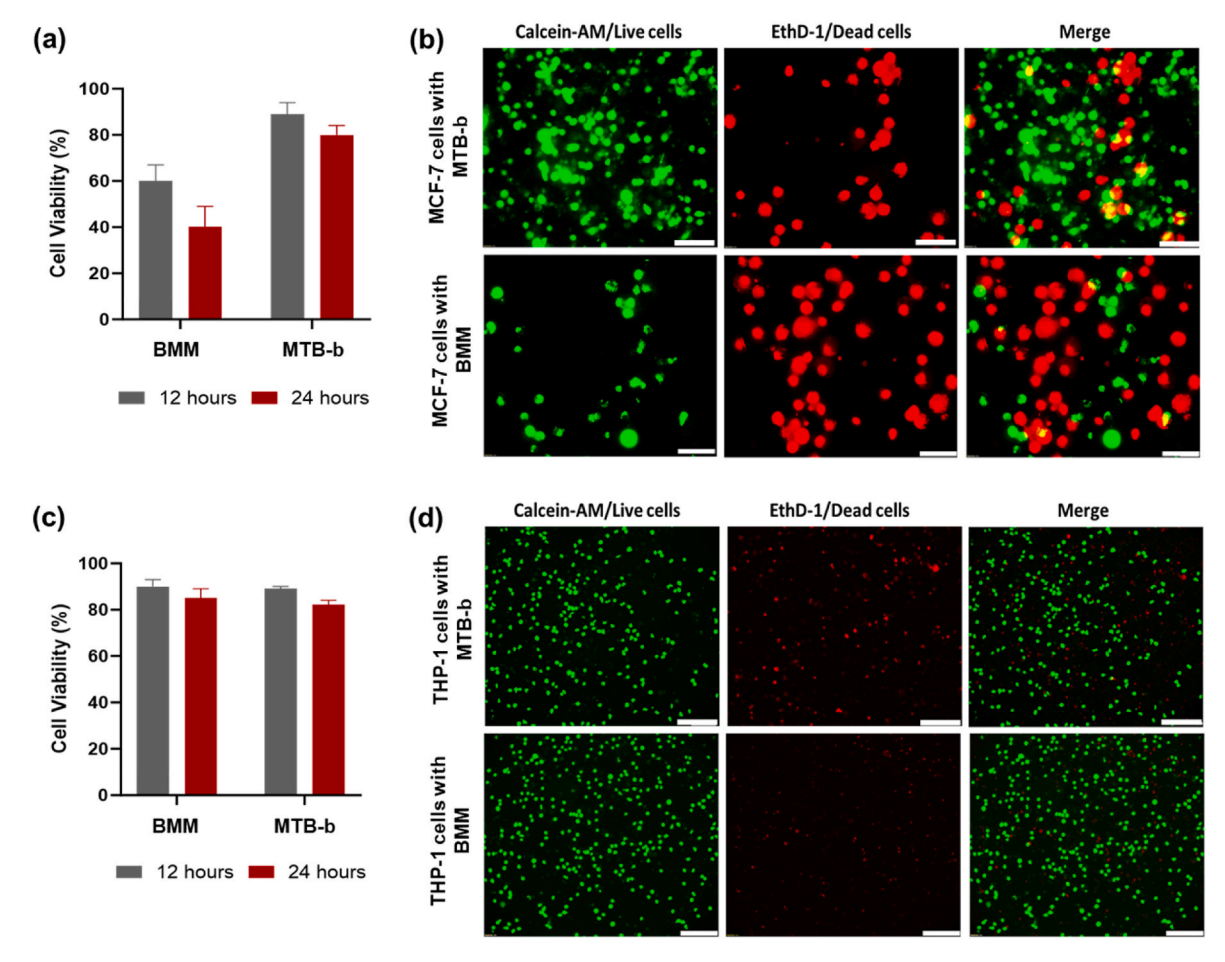


Fig. 8. Cell viability of MCF-7 and THP-1 upon drug release. (a) The viability of THP-1 cells after 12 and 24 h of incubation with BMM and MTB-b shows that around 80–90% of cells remained viable even after 24 h. (b) Fluorescence microscopy images display the Live/Dead cell viability of MCF-7 cells treated with BMM and MTB-b after 24 h of incubation. (c) When MCF-7 cells were treated with BMM, approximately 60% of the cells were killed after 24 h, whereas treatment with the MTB-b resulted in only 20–30% cell death. The error bars represent the mean \pm SD, n = 3. (d) Fluorescence microscopy images display the Live/Dead cell viability of THP-1 cells treated with BMM and MTB-b after 24 h of incubation. live cells emitted green fluorescence, while dead cells exhibited red fluorescence. Scale bar = 100 μ m.

dye, and its absorbance was measured using a microplate reader (BioTek Synergy H1) at 450 nm wavelength.

$2.8. \ \ \textit{Fluorescence visualization of different cell lines upon drug release}$

Fluorescence microscopy of various cell lines was performed to examine the effect of MTB-b and drug release from the BMM after 24 h of release. After incubating MCF-7 and THP-1 cells under optimal conditions, the cells were seeded in 96 well plates and treated with MTB-b and the BMM at the predetermined concentration and for the designated duration. After the incubation, the mixture was added with a Live/Dead cytotoxicity assay solution. Briefly, the cytotoxicity assay includes two different dyes namely, Ethidium homodimer-1 (EthD-1) and calcein-AM (Cal-AM). Initially, 20 μL of EthD-1 was dissolved in 10 mL of D-PBS, and then 5 μL of Cal-AM was added to the above 10 mL of EthD-1. Next, 10 μL of the freshly made Live/Dead solution was added to the mixture and incubated for 45 min at room temperature. The fluorescence images were acquired using an inverted microscope (OLYMPUS IX83).

2.9. Statistical analysis

Quantitative data were examined for statistical significance using a One-way ANOVA (GraphPad Prism version 10.0 software). A significant level of $p \leq 0.05$ was used for all tests.

3. Results and discussion

3.1. Design and characterization of BMM

The formation of the BMM was achieved through a three-step process involving a sandwiched reaction between MTB, PEG-biotin, and lenalidomide drug (Fig. 1). In the first step, the biotin-PEG-NHS reagent forms a strong bond with the MTB bacteria by leveraging the presence of free amine groups on their outer surfaces to acquire stealth properties (Fig. 2). During the drug delivery process, drug delivery devices often face the threat of attack by phagocytes, the process of PEGylation is employed to prevent recognition and uptake by endothelial cells in the blood as PEG is considered a potential stealth material [45,46]. Furthermore, the inclusion of PEG in the drug delivery devices enhances the solubility of drugs that are primarily hydrophobic in nature [47] and moreover, the use of biotin and NHS also plays a crucial role in the maintenance and bioconjugation processes. In many studies, biotin is considered a crucial vitamin essential for the proliferation and viability of bacterial cells [34] and it has been demonstrated to efficiently load and bind a variety of anticancer drugs through bioconjugation techniques [10].

The bacteria used in the given experiment are Gram-negative and helically shaped in nature with an average size of $0.3-0.5 \mu m$ in diameter and $1-2 \mu m$ in length. These bacteria also possess multiple internal chains of magnetic nanoparticles known as magnetosomes which direct the bacteria towards an external magnetic field. In the subsequent step,

the lenalidomide drug forms a robust bond with the biotin-PEG-NHS, capitalizing on the presence of primary amine groups within the structure of lenalidomide. In both coupling reactions, we harnessed the reactivity of NHS (N-Hydroxysuccinimide) groups within the biotin-PEG-NHS. These NHS groups react with primary amines, such as the amino termini of polypeptides or side chains of lysine or other functional groups within a compound's chemical structure. This reaction results in the formation of a robust amide bond through a nucleophilic attack while liberating the NHS group [48]. In the final step of the conjugation, a 100 μl of streptavidin solution was added to the MTB/PEG-biotin (MTB-b) and Lena/PEG-biotin complexes to create a link between the drug and the MTB. In this step, streptavidin utilizes the available free biotin from the previous couplings to establish a strong bond. Streptavidin has the ability to bind with high affinity to up to four biotin molecules [49]. Therefore, streptavidin forms a strong coupling bond with the biotin, resulting in the synthesis of a drug delivery BMM.

To confirm the successful attachment of the lenalidomide drug to the BMM, it was examined using a confocal laser scanning microscopy (CLSM) to verify the attachment of lenalidomide with the MTB-b (Fig. 3 (a)). The localization of the FITC-labeled BMM demonstrates a strong attachment of the drug to the drug carrier. In this context, the unlabeled MTB served as a control, enabling clear differentiation between the fluorescently labeled BMM and the bare MTB-b, which exhibited minimal or no fluorescence. In addition to fluorescence microscopic analysis, fluorescence-activated cell sorting (FACS) (Fig. 3(b)) was also performed, here, the samples were analyzed by comparing the monomodal fluorescence intensities of each specimen. The histograms indicate that the fluorescently labeled BMM has a higher and wider range of fluorescence intensity distribution compared to the unmodified MTB-b. The results were assessed through software (FlowJo) and it can be concluded from the result that more than 90% of MTB-b were conjugated with the drug.

FACS and confocal laser scanning microscopy (CLSM), an FT-IR measurement was also performed to validate the attachment of lenalidomide to the drug carrier. In Fig. 4, the FT-IR measurement of (a) PEG-Biotin and (b) PEG-Biotin-Lena are shown. The peak at 1648 cm⁻¹ indicates the carbonyl group (C=O) which is a prominent feature of biotin present in the PEG-biotin reagent, whereas the broad peak at 3446 cm indicates the presence of OH bond due to presence of water molecules as the PEG-biotin is prepared in the water. On the other hand, PEG-Biotin-Lena complex consists of a peak at 3473 cm⁻¹ which indicates NH stretches of primary amines, and a peak at 1438 cm⁻¹ shows aromatic C=C stretching vibration. Wavenumber 1670 cm⁻¹ indicates C=O stretching of the amide group and peaks at 1090 cm⁻¹ and 705 cm⁻¹ exhibit out-of-plane bending vibrations of the aromatic C-H. Along with FT-IR, the PEG-Biotin-LENA complex, with Lenalidomide (LENA) and PEG-Biotin, was analyzed using proton NMR Fig. 4(c). The PEG component predominantly exhibits peaks around 3.5 ppm, while Biotin shows characteristic peaks at approximately 6.5 ppm and 4.0 ppm [50]. Additionally, NHS presents a peak near 2.6 ppm [51]. The PEG-Biotin-LENA complex contains major peaks corresponding to both LENA and PEG-Biotin, confirming successful conjugation.

Moreover, to evaluate the magnetic mobility of the BMMs, we studied their movement in response to an external magnetic field. Fig. 5 (a) shows the demonstrated streamlined magnetic field generator using NdFeB permanent magnet (PM). The BMM solution was observed under a microscope within the PDMS wall, and the magnetic force was applied by controlling the distance between PM and the observation location. In the solution, as the BMM transfers along the magnetic force, drag force is exerted in the opposite direction of movement. The drag force exerted on the BMM can be estimated as an order of 10^{-14} N based on Stoke's law. To gain an appropriate magnetic force from the PM, we employed simulations to calculate the magnetic field distribution generated by the PM (dimensions: 4 mm \times 4 mm) according to the distance. Also, the intrinsic magnetization properties of the BMMs were measured (Fig. 5 (b)). By using the results of magnetic field simulation and BMM

magnetization, we calculated the magnetic force acting on the BMMs as a function of distance from the center of the PM surface (Fig. 5(c)). This indicates that the field generator provides enough magnetic force, which is over 10^{-13} N, to manipulate numerous BMM simultaneously against drag force resistance. Subsequently, we successfully navigated individual BMMs under the magnetic field gradient by approaching PM within 4 mm toward the BMM as shown in Fig. 5(d). The manipulated BMM exhibited directed trajectories that aligned with the direction of the applied magnetic force.

3.2. Analysis of bacterial viability with the lenalidomide drug

The viability of MTB upon the treatment with the lenalidomide drug was carried out utilizing a bacterial viability assay kit (Live/Dead Bac-Light). To obtain the desired results, the bacterial cells were treated with varying concentrations of lenalidomide at the given time intervals. The results obtained from this assay indicate that the bacteria treated with various concentrations of the drug did not significantly affect the viability of MTB even after a 24-h incubation (Fig. 6(a)). The results have been analyzed statistically. Based on the above observations, it can be concluded that varying concentrations of the drug, whether higher or lower, don't have a significant effect on bacterial viability even after an extended incubation period. This can be attributed to the fact that the present lenalidomide drug does not adversely affect bacterial viability over an extended period, suggesting that the MTB-b could be explored as a potential carrier for this drug in cancer treatment. Fig. 6(b), indicates a predominant presence of green-colored bacterial cells in comparison to the red-colored cells. Fig. 6(c), confirms that a significant number of bacterial cells remained viable even after a 24-h incubation with the drug. Fig. 6(d) displays a combined image of both live and dead bacteria.

3.3. pH-dependent release of the drug lenalidomide from the BMM

Fig. 7(a) shows the mechanism of releasing lenalidomide from the conjugated complex. In the acidic condition, the amide bond in the complex converses to carboxylic acid. It causes the elimination of an amine as a leaving group, releasing the lenalidomide. The solubility of lenalidomide is pH dependent, with higher solubility in acidic pH solutions, hence, the release of lenalidomide from the drug carried by BMM was assessed at 4 different pH values in PBS as shown in Fig. 7(b). In addition to the pH-dependent drug release, the process is also timedependent. At pH 7.4 a small amount of drug was released from the drug carrier during an incubation period of over 10 h, while a significant amount of drug was released when the pH of the solution was decreased to the pH value of 4.5. Most amount of drug approximately 2.3 µg/mL was released at around 20 h of incubation and after that time the drug release was controlled, illustrating that low pH could be a contributing factor to drug release from the drug carrier. Also, the conjugation of PEG-NHS-biotin with the lenalidomide drug makes it hydrophilic in nature, which in turn enhances its solubility.

3.4. Effect of BMM on different cell lines

Fig. 8 depicts the cell viability of (a) MCF-7 and (c) THP-1 cell lines following treatment with MTB-b and BMM at different incubation times (12 and 24 h) and this experiment was performed using an assay based on a cell counting kit-8 (CCK-8). The BMM was prepared by incubating it overnight with 50 μ g/mL of lenalidomide. THP-1 cell line is widely used in phagocytic assays as a human monocytic cell line [52]. Whereas MCF-7 is a human breast cancer cell line, and both the cell lines have different pH environments. MCF-7 cancer cells tend to acidify their environment, lowering the extracellular pH to approximately 5.7–7.8, whereas THP-1 monocytic cells maintain a neutral pH environment of around 7–7.6 for their proliferation [53,54]. In this assay, when THP-1 and MCF-7 cells were incubated with the MTB-b, minimal cell damage was observed, as this complex did not significantly affect the viability of

the cell lines. However, upon incubation with the BMM, it was observed that lenalidomide, driven by the different pH environments of the two cell types, caused more damage to the MCF-7 cancer cells. This effect was particularly pronounced since the extracellular environment of MCF-7 cells was more acidic compared to that of THP-1 cells.

Additionally, Fig. 8 displays the fluorescent microscopic images from the live/dead cell viability assay on both the (b) MCF-7 and (d) THP-1 cells after incubation with BMM and MTB-b. MCF-7 and THP-1 cells after getting treated with only drug carrier MTB-b for 24 h showed almost live states with green fluorescence. Because the drug carrier, composed of PEG-biotin and MTB, does not significantly affect the viability of both cell lines. When MCF-7 and THP-1 cells were incubated with the BMM, it is evident that almost 60% of MCF-7 cells were dead as shown in red fluorescence upon the release of the drug from the BMM. On the other hand, THP-1 cells displayed minimal loss of viability when incubated with BMM. This characteristic of the lenalidomide drug can be attributed to its lack of significant impact on the viability of THP-1 cells, as these cells are phagocytic and possess distinct properties compared to cancerous cells like MCF-7 cells [40].

4. Conclusion

In summary, the BMM presented here is an active drug delivery system comprising a live magnetotactic bacteria coupled with biotinylated polyethylene glycol loaded with the potent anticancer drug lenalidomide. This experimental work demonstrates the advantages of self-propelled magnetotactic bacteria, which possess small magnetic particles that enable facile manipulation using external magnetic fields, also they are primarily non-pathogenic in nature and hence can be used in both (in vitro and in vivo settings). Also, biotinylated PEG serves various purposes, including preserving bacterial viability, providing stealth properties to the drug delivery agent, enabling it to escape the phagocytic actions of the immune system, thereby allowing the drugs more time to reach and stay at the target area of interest. It also enhances the biodistribution of the drug and increases the solubility of the lenalidomide drug, which is primarily a hydrophobic material. The release of the drug was triggered by the low pH environment found in cancer cell lines. Therefore, the proposed BMM can be used as a potential drug delivery system, demonstrating precise targeting, stealth properties, and pH-triggered drug release within the acidic environments of cancer cells. The upcoming experiments will be directed towards enhancing the effectiveness of the drug delivery system by investigating other essential drugs such as antibiotics, cardiovascular drugs, and other cancer drugs. These studies will also explore their performance in blood vessels, tumors, and bacterial biofilms.

CRediT authorship contribution statement

Richa Chaturvedi: Writing – original draft, Methodology, Investigation, Conceptualization. Yumin Kang: Methodology, Investigation. Yunji Eom: Methodology. Sri Ramulu Torati: Writing – review & editing, Investigation, Formal analysis, Conceptualization. CheolGi Kim: Supervision, Funding acquisition, Conceptualization.

Declaration of competing interest

The authors declare that they have no known competing financial interests or personal relationships that could have appeared to influence the work reported in this paper.

The author is an Editorial Board Member/Editor-in-Chief/Associate Editor/Guest Editor for *Journal of Science: Advanced Materials and Devices* and was not involved in the editorial review or the decision to publish this article.

Acknowledgements

This research was supported by the National Research Foundation of Korea (NRF) grant funded by the Korean government (MSIT) (2018R1A5A1025511).

References

- W. You, M. Henneberg, Cancer Incidence Increasing Globally: the Role of Relaxed Natural Selection, vol. 11, 2018, pp. 140–152, https://doi.org/10.1111/ eva 12523
- [2] Y.H. Bae, Drug targeting and tumor heterogeneity, J. Contr. Release 133 (2009) 2–3, https://doi.org/10.1016/j.jconrel.2008.09.074.
- [3] M.U. Naidu, G.V. Ramana, P.U. Rani, I.K. Mohan, A. Suman, P. Roy, Chemotherapy-induced and/or radiation therapy-induced oral mucositiscomplicating the treatment of cancer, Neoplasia 6 (2004) 423–431, https://doi. org/10.1593/neo.04169
- [4] K.H. Bae, H.J. Chung, T.G. Park, Nanomaterials for cancer therapy and imaging, Mol. Cells 31 (2011) 295–302, https://doi.org/10.1007/s10059-011-0051-5.
- [5] S. Bae, K. Ma, T.H. Kim, E.S. Lee, K.T. Oh, E.S. Park, K.C. Lee, Y.S. Youn, Doxorubicin-loaded human serum albumin nanoparticles surface-modified with TNF-related apoptosis-inducing ligand and transferrin for targeting multiple tumor types, Biomaterials 33 (2012) 1536–1546, https://doi.org/10.1016/j. biomaterials.2011.10.050.
- [6] P.N. Navya, A. Kaphle, H.K. Daima, Nanomedicine in sensing, delivery, imaging and tissue engineering: advances, opportunities and challenges, in: P.J. Thomas, N. Revaprasadu (Eds.), Nanoscience, vol. 5, The Royal Society of Chemistry, 2018, pp. 30–56.
- [7] Z. Cheng, M. Li, R. Dey, Y. Chen, Nanomaterials for cancer therapy: current progress and perspectives, J. Hematol. Oncol. 14 (2021) 85, https://doi.org/ 10.1186/s13045-021-01096-0.
- [8] M. Chidambaram, R. Manavalan, K. Kathiresan, Nanotherapeutics to overcome conventional cancer chemotherapy limitations, J. Pharm. Pharmaceut. Sci. 14 (2011) 67–77, https://doi.org/10.18433/j30c7d.
- [9] T.M. Allen, P.R. Cullis, Drug Delivery Systems: Entering the Mainstream, vol. 303, 2004, pp. 1818–1822, https://doi.org/10.1126/science.1095833.
- [10] S. Park, E. Kim, W.Y. Kim, C. Kang, J.S. Kim, Biotin-guided anticancer drug delivery with acidity-triggered drug release, Chem. Commun. 51 (2015) 9343–9345, https://doi.org/10.1039/C5CC03003J.
- [11] D. Liu, F. Yang, F. Xiong, N. Gu, The smart drug delivery system and its clinical potential, Theranostics 6 (9) (2016) 1306–1323, https://doi.org/10.7150/ thpo.14858
- [12] A.K. Pandya, L.K. Vora, C. Umeyor, D. Surve, A. Patel, S. Biswas, K. Patel, V. B. Patravale, Polymeric in situ forming depots for long-acting drug delivery systems, Adv. Drug Deliv. Rev. 200 (2023 Sep) 115003, https://doi.org/10.1016/j.addr.2023.115003.
- [13] Morteza Rabiei, Soheila Kashanian, Seyedeh Sabereh Samavati, Hossein Derakhshankhah, Shahriar Jamasb, Steven JP. McInnes, Nanotechnology application in drug delivery to osteoarthritis (OA), rheumatoid arthritis (RA), and osteoporosis (OSP), J. Drug Deliv. Sci. Technol. 61 (2021) 102011, https://doi. org/10.1016/j.jddst.2020.102011.
- [14] Mary Sajini Devadas, et al., Synthesis and characterization of magnetoplasmonic air-stable Au@ FeCo, Langmuir 39 (5) (2023) 1947–1956, https://doi.org/ 10.1021/acs.langmuir.2c02965.
- [15] A. Baelo, R. Levato, E. Julián, A.V. Crespo, J. Astola, J. Gavaldà, E. Engel, M. A. Mateos-Timoneda, E. Torrents, Disassembling Bacterial Extracellular Matrix with DNase-Coated Nanoparticles to Enhance Antibiotic Delivery in Biofilm Infections, vol. 209, 2015, pp. 150–158, https://doi.org/10.1016/j.iconrel.2015.04.028.
- [16] J. Li, B. Esteban-Fernández de Ávila, W. Gao, L. Zhang, J. Wang, Micro/nanorobots for Biomedicine: Delivery, Surgery, Sensing, and Detoxification, vol. 2, 2017, https://doi.org/10.1126/scirobotics.aam6431 eaam6431.
- [17] S. Suh, A. Jo, M.A. Traore, Y. Zhan, S.L. Coutermarsh-Ott, V.M. Ringel-Scaia, I. C. Allen, R.M. Davis, B. Behkam, Nanoscale Bacteria-Enabled Autonomous Drug Delivery System (NanoBEADS) Enhances Intratumoral Transport of Nanomedicine, vol. 6, 2019 1801309, https://doi.org/10.1002/advs.201801309.
- [18] M.T.-Q. Duong, Y. Qin, S.-H. You, J.-J. Min, Bacteria-cancer interactions: bacteria-based cancer therapy, Exp. Mol. Med. 51 (2019) 1–15, https://doi.org/10.1038/s12276-019-0297-0.
- [19] Z. Cao, J. Liu, Bacteria and bacterial derivatives as drug carriers for cancer therapy, J. Contr. Release: official journal of the Controlled Release Society 326 (2020) 396–407, https://doi.org/10.1016/j.jconrel.2020.07.009.
- [20] N.S. Forbes, Engineering the perfect (bacterial) cancer therapy, Nat. Rev. Cancer 10 (2010) 785–794, https://doi.org/10.1038/nrc2934.
- [21] Y.-J. Xie, M. Huang, D. Li, J.-C. Hou, H.-H. Liang, A.A. Nasim, J.-M. Huang, C. Xie, E.L.-H. Leung, X.-X. Fan, Bacteria-based nanodrug for anticancer therapy, Pharmacol. Res. 182 (2022) 106282, https://doi.org/10.1016/j. phrs.2022.106282.
- [22] B.J. Williams, S.V. Anand, J. Rajagopalan, M.T.A. Saif, A self-propelled biohybrid swimmer at low Reynolds number, Nat. Commun. 5 (2014) 3081, https://doi.org/ 10.1038/ncomms4081.
- [23] S. Xie, P. Zhang, Z. Zhang, Y. Liu, M. Chen, S. Li, X. Li, Bacterial navigation for tumor targeting and photothermally-triggered bacterial ghost transformation for

- spatiotemporal drug release, Acta Biomater. 131 (2021) 172–184, https://doi.org/10.1016/j.actbio.2021.06.030.
- [24] S. Patyar, R. Joshi, D.S.P. Byrav, A. Prakash, B. Medhi, B.K. Das, Bacteria in cancer therapy: a novel experimental strategy, J. Biomed. Sci. 17 (2010) 21, https://doi. org/10.1186/1423-0127-17-21.
- [25] O. Felfoul, M. Mohammadi, S. Taherkhani, D. de Lanauze, Y. Zhong Xu, D. Loghin, S. Essa, S. Jancik, D. Houle, M. Lafleur, L. Gaboury, M. Tabrizian, N. Kaou, M. Atkin, T. Vuong, G. Batist, N. Beauchemin, D. Radzioch, S. Martel, Magneto-aerotactic bacteria deliver drug-containing nanoliposomes to tumour hypoxic regions, Nat. Nanotechnol. 11 (2016) 941–947, https://doi.org/10.1038/ nnano.2016.137.
- [26] Y. Liu, W. Wang, J. Yang, C. Zhou, J. Sun, pH-sensitive polymeric micelles triggered drug release for extracellular and intracellular drug targeting delivery, Asian J. Pharm. Sci. 8 (2013) 159–167, https://doi.org/10.1016/j. aips.2013.07.021.
- [27] J. Xing, T. Yin, S. Li, T. Xu, A. Ma, Z. Chen, Y. Luo, Z. Lai, Y. Lv, H. Pan, R. Liang, X. Wu, M. Zheng, L. Cai, Sequential Magneto-Actuated and Optics-Triggered Biomicrorobots for Targeted Cancer Therapy, vol. 31, 2021 2008262, https://doi.org/10.1002/adfm.202008262.
- [28] S. Rismani Yazdi, P. Agrawal, E. Morales, C.A. Stevens, L. Oropeza, P.L. Davies, C. Escobedo, R.D. Oleschuk, Facile actuation of aqueous droplets on a superhydrophobic surface using magnetotactic bacteria for digital microfluidic applications, Anal. Chim. Acta 1085 (2019) 107–116, https://doi.org/10.1016/j. 202 2010 08 020
- [29] N. Mirkhani, M.G. Christiansen, S. Schuerle, Living, Self-Replicating Ferrofluids for Fluidic Transport 30 (2020) 2003912, https://doi.org/10.1002/adfm.202003912.
- [30] K.G. Gareev, D.S. Grouzdev, P.V. Kharitonskii, A. Kosterov, V.V. Koziaeva, E. S. Sergienko, M.A. Shevtsov, Magnetotactic Bacteria and Magnetosomes, vol. 7, Basic Properties and Applications, 2021, p. 86, https://doi.org/10.3390/magnetochemistry7060086.
- [31] E. Masoudipour, S. Kashanian, A.H. Azandaryani, et al., Surfactant effects on the particle size, zeta potential, and stability of starch nanoparticles and their use in a pH-responsive manner, Cellulose 24 (2017) 4217–4234, https://doi.org/10.1007/ s10570-017-1426-3.
- [32] M. Motiei, S. Kashanian, A. (Arman). Taherpour, Hydrophobic amino acids grafted onto chitosan: a novel amphiphilic chitosan nanocarrier for hydrophobic drugs, Drug Dev. Ind. Pharm. 43 (1) (2016) 1–11, https://doi.org/10.1080/ 03639045.2016.1254240.
- [33] J. Silvestre, C. Delattre, P. Michaud, H. de Baynast, Optimization of chitosan properties with the aim of a water resistant adhesive development, Polymers 13 (2021) 4031, https://doi.org/10.3390/polym13224031.
- [34] H.P. Broquist, E.E. Snell, Biotin and bacterial growth. I. Relation to aspartate, oleate, and carbon dioxide, J. Biol. Chem. 188 (1951) 431–444, https://doi.org/ 10.1016/S0021-9258(18)56187-1.
- [35] S. Zhu, Y. Cheng, J. Wang, G. Liu, T. Luo, X. Li, S. Yang, R. Yang, Biohybrid magnetic microrobots: an intriguing and promising platform in biomedicine, Acta Biomater. 169 (2023) 88–106, https://doi.org/10.1016/j.actbio.2023.08.005.
- [36] J. Xing, T. Yin, S. Li, T. Xu, A. Ma, Z. Chen, Y. Luo, Z. Lai, Y. Lv, H. Pan, R. Liang, X. Wu, M. Zheng, L. Cai, Sequential Magneto-Actuated and Optics-Triggered Biomicrorobots for Targeted Cancer Therapy, vol. 31, 2021 2008262, https://doi.org/10.1002/adfm.202008262.
- [37] V. Kotla, S. Goel, S. Nischal, C. Heuck, K. Vivek, B. Das, A. Verma, Mechanism of action of lenalidomide in hematological malignancies, J. Hematol. Oncol. 2 (2009) 36, https://doi.org/10.1186/1756-8722-2-36.

- [38] Z. Lin, Y. Amako, F. Kabir, H.A. Flaxman, B. Budnik, C.M. Woo, Development of photolenalidomide for cellular target identification, J. Am. Chem. Soc. 144 (2022) 606–614, https://doi.org/10.1021/jacs.1c11920.
- [39] E. Crane, A. List, Lenalidomide: an immunomodulatory drug, Future Oncol. 1 (2005) 575–583, https://doi.org/10.2217/14796694.1.5.575.
- [40] Jessica M. McDaniel, Javier Pinilla-Ibarz, P.K. Epling-Burnette, Molecular action of lenalidomide in lymphocytes and hematologic malignancies, Advances in Hematology 9 (2012) 513702, https://doi.org/10.1155/2012/513702, 2012.
- [41] L.L. Yin, X.M. Wen, Q.H. Lai, J. Li, X.W. Wang, Lenalidomide improvement of cisplatin antitumor efficacy on triple-negative breast cancer cells in vitro, Oncol. Lett. 15 (5) (2018 May) 6469–6474, https://doi.org/10.3892/ol.2018.8120.
- [42] R. Chaturvedi, Y. Kang, Y. Eom, S.R. Torati, C. Kim, Functionalization of Biotinylated Polyethylene Glycol on Live Magnetotactic Bacteria Carriers for Improved Stealth Properties, vol. 10, 2021, p. 993, https://doi.org/10.3390/ biology10100993.
- [43] C. Zahn, S. Keller, M. Toro-Nahuelpan, P. Dorscht, W. Gross, M. Laumann, S. Gekle, W. Zimmermann, D. Schüler, H. Kress, Measurement of the magnetic moment of single Magnetospirillum gryphiswaldense cells by magnetic tweezers, Sci. Rep. 7 (2017) 3558, https://doi.org/10.1038/s41598-017-03756-z.
- [44] R.N. Herqash, F.A. Alkathiri, I.A. Darwish, Assessing pharmacokinetics and drugdrug interactions of the combination therapy of myelofibrosis with ruxolitinib and lenalidomide by a new eco-friendly HPLC method for their simultaneous determination in plasma, Cancer Chemother. Pharmacol. 94 (2024) 747–761, https://doi.org/10.1007/s00280-024-04715-y.
- [45] W.J. Kelley, C.A. Fromen, G. Lopez-Cazares, O. Eniola-Adefeso, PEGylation of model drug carriers enhances phagocytosis by primary human neutrophils, Acta Biomater. 79 (2018) 283–293, https://doi.org/10.1016/j.actbio.2018.09.001.
- [46] M.D. Howard, M. Jay, T.D. Dziubla, X. Lu, PEGylation of nanocarrier drug delivery systems: state of the art, J. Biomed. Nanotechnol. 4 (2008) 133–148, https://doi. org/10.1166/jbn.2008.021.
- [47] F.M. Veronese, A. Mero, The impact of PEGylation on biological therapies, BioDrugs: clinical immunotherapeutics, biopharmaceuticals and gene therapy 22 (2008) 315–329, https://doi.org/10.2165/00063030-200822050-00004.
- [48] G.T. Hermanson, Bioconjugate Techniques, third ed., Academic Press, Boston, 2013.
- [49] C.M. Dundas, D. Demonte, S. Park, Streptavidin-biotin technology: improvements and innovations in chemical and biological applications, Appl. Microbiol. Biotechnol. 97 (2013) 9343–9353, https://doi.org/10.1007/s00253-013-5232-z.
- [50] S.Y. Kim, S.H. Cho, Y.M. Lee, et al., Biotin-conjugated block copolymeric nanoparticles as tumor-targeted drug delivery systems, Macromol. Res. 15 (2007) 646–655, https://doi.org/10.1007/BF03218945.
- [51] R.P. Chauhan, G. Singh, S. Singh, et al., Biotinylated magnetic nanoparticles for pretargeting: synthesis and characterization study, Cancer Nano 2 (2011) 111–120, https://doi.org/10.1007/s12645-011-0021-9.
- [52] M.E. Ackerman, B. Moldt, R.T. Wyatt, A.S. Dugast, E. McAndrew, S. Tsoukas, S. Jost, C.T. Berger, G. Sciaranghella, Q. Liu, D.J. Irvine, D.R. Burton, G. Alter, A robust, high-throughput assay to determine the phagocytic activity of clinical antibody samples, J. Immunol. Methods 366 (2011) 8–19, https://doi.org/ 10.1016/j.ijm.2010.12.016.
- [53] S. Lee, A. Shanti, Effect of exogenous pH on cell growth of breast cancer cells, Int. J. Mol. Sci. 22 (2021), https://doi.org/10.3390/ijms22189910.
- [54] B.A. Webb, M. Chimenti, M.P. Jacobson, D.L. Barber, Dysregulated pH: a perfect storm for cancer progression, Nat. Rev. Cancer 11 (2011) 671–677, https://doi. org/10.1038/nrc3110.